Dyes and Pigments 87 (2010) 22–29

Contents lists available at ScienceDirect

Dyes and Pigments

journal homepage: www.elsevier.com/locate/dyepig

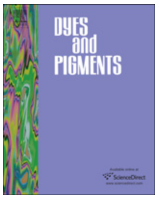

The synthesis of chiral, cationic nonlinear optical dyes based on the 1,1′-binaphthalenyl unit

Benjamin J. Coe [a,*], Elizabeth C. Harper [a], Koen Clays [b], Edith Franz [b]

[a] *School of Chemistry, University of Manchester, Oxford Road, Manchester M13 9PL, UK*
[b] *Department of Chemistry, University of Leuven, Celestijnenlaan 200D, B-3001 Leuven, Belgium*

ARTICLE INFO

Article history:
Received 14 December 2009
Received in revised form
22 January 2010
Accepted 25 January 2010
Available online 18 February 2010

Keywords:
Organic salts
Nonlinear optics
Hyper-Rayleigh scattering
Chirality

ABSTRACT

The *R* enantiomers of three, novel, 2D dipolar cations with 2,2′-bis(dimethylamino)-1,1′-binaphthalenyl electron donor groups connected to *N*-R-pyridinium acceptors were synthesised. The compounds displayed intense intramolecular charge-transfer bands in the visible region, the maximal energy of which decreased as R changed in the order Me > 2,4-dinitrophenyl > 2-pyrimidyl. Molecular quadratic nonlinear optical responses were determined for the chloride salts in methanol using femtosecond, hyper-Rayleigh scattering with 1300 and 800 nm lasers. The measured first hyperpolarizabilities β_{HRS} were in the range 34–155 × 10^{-30} esu and increased at both wavelengths, showing the expected inverse relationship with respect to the charge-transfer energies. Single crystal X-ray structures were determined for the precursor compounds (*R*)-6,6′-dibromo-2,2′-bis(dimethylamino)-1,1′-binaphthalenyl and (*R*)-2,2′-bis(dimethylamino)-1,1′-binaphthalenyl-6,6′-dicarbaldehyde, revealing an average dihedral angle between the naphthalenyl units of 73°. Making the assumption that this angle was similar to that found in the chromophores studies in solution allowed the determination of two independent tensor components, β_{zzz} and β_{zxx}. For these molecules the greatest proportion of the total first hyperpolarizability lay along the charge-transfer axis (β_{zzz}), but the “off-diagonal” β_{zxx} values were still substantial (31–141 × 10^{-30} esu) and larger when compared with those determined by hyper-Rayleigh scattering for other 2D dipoles in the literature.

1. Introduction

There is continued interest in the synthesis and study of molecular nonlinear optical (NLO) materials, primarily inspired by various potential applications such as optical data processing and biological imaging [1]. Although most organic NLO compounds are charge neutral, salts are especially promising due to their often high stabilities and synthetic tailorability. By varying the counterion accompanying an active charged chromophore, it is possible to modify crystal packing arrangements to produce polar structures showing bulk quadratic NLO effects such as second harmonic generation (SHG) and electro-optic (EO) behaviour. Much attention has focused on stilbazolium species, especially (*E*)-4′-(dimethylamino)-*N*-methyl-4-stilbazolium tosylate (DAST) [2] and closely related compounds [3]. Because of their large EO coefficients, such materials are useful for terahertz (THz) wave generation via nonlinear frequency mixing, of relevance to a range of applications including security scanning, biomedical analysis and space communications [4].

One approach to producing polar materials with some degree of control is to incorporate chirality into either the active chromophore or the accompanying ions if the compound is a salt. Resolved chiral species must inevitably crystallise noncentrosymmetrically, although it is noteworthy that this does not guarantee that the molecular dipoles will align favourably. This strategy has been adopted successfully with stilbazolium compounds by Andreu et al. who produced a chromophore bearing a 2-(methoxymethyl)pyrrolidinyl substituent which packs in the space group $P2_1$ and gives a large powder SHG response of 80 times a urea standard (measured using a 1907 nm laser) [5]. The 1,1′-binaphthalenyl unit is a convenient chiral motif that has been incorporated into various neutral NLO compounds [6], including polymeric materials [6f–k] and also some charged organometallic species [7]. Very recently, Yan et al. reported a dicationic 1,1′-binaphthalenyl chromophore for use as a probe for imaging cell membranes via resonance-enhanced SHG [8], although the molecular-level NLO properties of this species were not described. Previous studies in our laboratory have shown that the static first hyperpolarizabilities β_0 (the origin of quadratic NLO effects) of stilbazolium

---

* Corresponding author. Tel.: +44 161 275 4601; fax: +44 161 275 4598.
E-mail address: b.coe@manchester.ac.uk (B.J. Coe).

0143-7208/$ – see front matter © 2010 Elsevier Ltd. All rights reserved.
doi:10.1016/j.dyepig.2010.01.018

and related chromophores can be increased considerably by replacing the commonly used *N*-alkylpyridinium electron acceptors with *N*-aryl units [9]. This work has produced two new materials showing powder SHG activities similar to that of DAST (*ca.* 500 times urea at 1907 nm) [9a,c]. In addition, large single crystals of the compound (*E*)-4′-(dimethylamino)-*N*-phenyl-4-stilbazolium hexafluorophosphate (DAPSH) show a record non-resonant bulk NLO coefficient d_{111} of 290 pm V^{-1} at 1907 nm [10]. In this report, we disclose preliminary investigations into the synthesis of 1,1′-binaphthalenyl derivatives containing *N*-arylpyridinium groups and their study by using the hyper-Rayleigh scattering (HRS) technique [11].

2. Experimental

2.1. Materials and procedures

The compound (*R*)-6,6′-dibromo-1,1′-binaphthalenyl-2,2′-diamine (**1**) was prepared according to a published procedure [8]. Tetrahydrofuran was dried over sodium and triethylamine was dried over CaH_2, and both were freshly distilled before use. 4-Vinylpyridine was obtained commercially and fractionally distilled prior to use. All other reagents were obtained commercially and used as supplied. Products were dried overnight at room temperature in a vacuum desicator ($CaSO_4$) prior to characterisation.

2.2. General physical measurements

^{1}H NMR spectra were recorded on an Inova 400 (compounds **2** and **3**) or a Bruker UltraShield 500 (all other compounds) spectrometer and all shifts are quoted with respect to TMS. The fine splitting of aryl ring AA′BB′ patterns is ignored and the signals are reported as simple doublets, with *J* values referring to the two most intense peaks. Elemental analyses were performed by the Microanalytical Laboratory, University of Manchester. IR spectra were obtained as KBr discs with an ATI Mattson Genesis Series FTIR instrument, and mass spectra were measured using +electrospray on a Micromass Platform II spectrometer with acetonitrile as the solvent.

2.3. Synthesis

2.3.1. (R)-6,6′-Dibromo-2,2′-bis(dimethylamino)-1,1′-binaphthalenyl, 2

To 20% aqueous H_2SO_4 (0.65 mL) and 40% aqueous formaldehyde (0.35 mL) in THF (1 mL) at 0 °C were added simultaneously a solution of **1** (150 mg, 0.339 mmol) in THF (8 mL) and $NaBH_4$ (188 mg, 4.97 mmol). Once the addition was complete, the solution was allowed to warm to room temperature and stirred for 70 min. It was then poured into 2% aqueous KOH (32 mL), and the organic layer was extracted with ethyl acetate and dried ($MgSO_4$). The extracts were combined and concentrated under reduced pressure to afford a yellow-brown solid (170 mg). This material was purified by using column chromatography on silica gel with 99:1 *n*-hexane/ethyl acetate as the eluant. The first fraction was collected and evaporated to dryness under reduced pressure to afford a yellow powder. Yield 86 mg (51%). δ_H ($CDCl_3$) 7.95 (d, 2H, *J* = 2.2 Hz, $C_{10}H_5$), 7.77 (d, 2H, *J* = 9.2 Hz, $C_{10}H_5$), 7.45 (d, 2H, *J* = 8.8 Hz, $C_{10}H_5$), 7.23 (dd, 2H, *J* = 9.1, 1.9 Hz, $C_{10}H_5$), 6.98 (d, 2H, *J* = 9.2 Hz, $C_{10}H_5$), 2.47 (s, 12H, Me). *m/z* = 499 ($[C_{24}H_{22}Br^{79}Br^{81}N_2 + H]^+$), 497 ($[C_{24}H_{22}Br^{79}Br^{79}N_2 + H]^+$), 501 ($[C_{24}H_{22}Br^{81}Br^{81}N_2 + H]^+$). Anal. Calcd (%) for $C_{24}H_{22}Br_2N_2$: C, 57.85; H, 4.45; N, 5.62. Found: C, 57.78; H, 4.46; N, 5.47. Diffraction-quality crystals were grown by slow evaporation of a 99:1 *n*-hexane/ethyl acetate solution.

2.3.2. (R)-2,2′-Bis(dimethylamino)-1,1′-binaphthalenyl-6,6′-dicarbaldehyde, 3

To a solution of **2** (200 mg, 0.401 mmol) in dry THF (15 mL) under an argon atmosphere was added dropwise *n*-butyllithium (1.6 M in hexanes; 0.8 mL, 1.28 mmol) at −78 °C; the pale yellow solution turned deep red and then green-yellow and was stirred for 40 min at −78 °C. Dry DMF (0.3 mL, 3.87 mmol) was added dropwise at −78 °C and the reaction stirred for 10 min, then the solution was allowed to warm to room temperature and stirred for a further 3 h. The orange solution was poured into water (20 mL) and the organic layer extracted with ethyl acetate and dried ($MgSO_4$). The extracts were combined and concentrated under reduced pressure to afford a yellow solid (150 mg). Purification was effected by using column chromatography on silica gel with 7:3 *n*-hexane/ethyl acetate as the eluant. The first fraction was collected and evaporated to dryness under reduced pressure to afford a yellow powder. Yield 90 mg (55%). δ_H ($CDCl_3$) 10.07 (s, 2H, CHO), 8.29 (s, 2H, $C_{10}H_5$), 8.00 (d, 2H, *J* = 8.9 Hz, $C_{10}H_5$), 7.65 (d, 2H, *J* = 8.9 Hz, $C_{10}H_5$), 7.46 (d, 2H, *J* = 9.2 Hz, $C_{10}H_5$), 7.22 (d, 2H, *J* = 8.8 Hz, $C_{10}H_5$), 2.55 (s, 12H, Me). *m/z* = 419 ($[M + Na]^+$). υ(C=O) 1668 s cm^{-1}. Anal. Calcd (%) for $C_{26}H_{24}N_2O_2 \bullet 0.7H_2O$: C, 76.33; H, 6.26; N, 6.85. Found: C, 76.32; H, 5.95; N, 6.67. Diffraction-quality crystals were grown by vapour diffusion of *n*-hexane into an ethyl acetate solution.

2.3.3. (R)-6,6′-Bis-((E)-2-(pyridin-4-yl)vinyl)-2,2′-bis(dimethylamino)-1,1′-binaphthalenyl, 4

Working in a glove box, **2** (120 mg, 0.241 mmol), $Pd(OAc)_2$ (72 mg, 0.321 mmol) and tri-*ortho*-tolylphosphine (146 mg, 0.480 mmol) were placed in a sealed pressure vessel. To this mixture was added triethylamine (5 mL) and 4-vinylpyridine (1.65 mL, 15.4 mmol) and the vessel was sealed tightly. The reaction was stirred at 110 °C for 16 h; initially the colour changed from pale yellow to bright orange, and the solution was then allowed to cool to room temperature. The Pd black formed was removed using a short column on silica gel with 1:1 dichloromethane/methanol as the eluant, and the solvents were evaporated to give a red oily solid. This material was further purified using column chromatography on silica gel with ethyl acetate as the eluant to give separation and then 1:1 ethyl acetate/methanol to bring off the product. The first major orange band was collected and evaporated to dryness under reduced pressure. Further purification was achieved by vapour diffusion of *n*-pentane into a chloroform solution, affording a yellow microcrystalline solid. Yield: 70 mg (50%). δ_H ($CDCl_3$) 8.56 (d, 4H, *J* = 6.0 Hz, C_5H_4N), 7.90–7.88 (4H, $C_{10}H_5$), 7.47–7.36 (6H, CH and $C_{10}H_5$), 7.37 (d, 4H, *J* = 6.0 Hz, C_5H_4N), 7.19 (d, 2H, *J* = 9.1 Hz, $C_{10}H_5$), 7.02 (d, 2H, *J* = 16.1 Hz, CH), 2.52 (s, 12H, Me). *m/z* = 548 ($[M + H]^+$). Anal. Calcd (%) for $C_{38}H_{34}N_4 \bullet 1/3CHCl_3$: C, 78.50; H, 5.90; N, 9.55. Found: C, 78.69; H, 6.13; N, 9.57. After heating for 24 h under vacuum: Anal. Calcd (%) for $C_{38}H_{34}N_4 \bullet 1/5CHCl_3$: C, 80.41; H, 6.04; N, 9.82. Found: C, 80.74; H, 5.84; N, 9.71. After heating for a further 3 d under vacuum: Anal. Calcd (%) for $C_{38}H_{34}N_4 \bullet 1/8CHCl_3$: C, 81.53; H, 6.12; N, 9.98. Found: C, 81.62; H, 5.63; N, 9.92.

2.3.4. (R)-6,6′-Bis-((E)-2-(1-methylpyridin-4-yl)vinyl)-2,2′-bis(dimethylamino)-1,1′-binaphthalenyl Iodide, [5]I$_2$

To a solution of **4**•1/8$CHCl_3$ (41 mg, 0.073 mmol) in acetone (12 mL) was added MeI (0.01 mL). The reaction was heated under reflux in the dark for 4 h, and a red precipitate began to form after 1 h. After cooling to room temperature, the solid was filtered off, washed with diethyl ether and dried. Yield: 52 mg (79%). δ_H (CD_3OD) 8.67 (d, 4H, *J* = 7.1 Hz, C_5H_4N), 8.15–8.13 (6H, C_5H_4N and $C_{10}H_5$), 8.07 (d, 2H, *J* = 16.1 Hz, CH), 8.01 (d, 2H, *J* = 8.8 Hz, $C_{10}H_5$), 7.64 (dd, 2H, *J* = 9.0, 2.0 Hz, $C_{10}H_5$), 7.57 (d, 2H, *J* = 9.1 Hz, $C_{10}H_5$), 7.41 (d, 2H, *J* = 15.9 Hz, CH), 7.17 (d, 2H, *J* = 8.8 Hz, $C_{10}H_5$), 4.30 (s, 6H, N^+–Me), 2.56 (s, 12H, Me). *m/z* = 288 ($[M - 2I]^{2+}$). Anal. Calcd

(%) for $C_{40}H_{40}I_2N_4{\bullet}4H_2O$: C, 53.23; H, 5.36; N, 6.21. Found: C, 53.08; H, 5.04; N, 6.15.

2.3.5. *(R)-6,6′-Bis-((E)-2-(1-(2,4-dinitrophenyl)pyridin-4-yl)vinyl)-2,2′-bis(dimethylamino)-1,1′-binaphthalenyl Chloride, [**6**]Cl₂*

To a solution of **4**•1/8CHCl₃ (20 mg, 0.036 mmol) in 2-butanone (6 mL) was added 2,4-dinitrochlorobenzene (296 mg, 1.46 mmol). The reaction was heated under reflux in the dark for 24 h, after which time the solution was colourless with a black precipitate. After cooling to room temperature, the solid was filtered off, washed with 2-butanone then diethyl ether and dried. Yield: 26 mg (72%). δ_H (CD_3OD) 9.26 (d, 2H, J = 2.5 Hz, PhH^3), 8.96 (d, 4H, J = 7.1 Hz, C_5H_4N), 8.90 (dd, 2H, J = 8.8, 2.5 Hz, PhH^5), 8.38–8.26 (10H, CH, C_5H_4N, PhH^6 and $C_{10}H_5$), 8.06 (d, 2H, J = 9.1 Hz, $C_{10}H_5$), 7.73 (d, 2H, J = 9.1 Hz, $C_{10}H_5$), 7.60–7.55 (4H, CH and $C_{10}H_5$), 7.21 (d, 2H, J = 8.8 Hz, $C_{10}H_5$), 2.61 (s, 12H, Me). m/z = 441 ($[M - 2Cl]^{2+}$). Anal. Calcd (%) for $C_{50}H_{40}Cl_2N_8O_8{\bullet}3H_2O$: C, 59.70; H, 4.61; N, 11.14. Found: C, 59.73; H, 4.72; N, 10.70.

2.3.6. *(R)-6,6′-Bis-((E)-2-(1-(2-pyrimidyl)pyridin-4-yl)vinyl)-2,2′-bis(dimethylamino)-1,1′-binaphthalenyl Iodide, [**7**]I₂*

To a solution of **4**•1/8CHCl₃ (40 mg, 0.071 mmol) in 2-butanone (12 mL) was added 2-chloropyrimidine (38 mg, 0.332 mmol). The reaction was heated under reflux in the dark for 17 h, after which time the solution was colourless with a dark purple precipitate. After cooling to room temperature, the solid was filtered off, washed with 2-butanone then diethyl ether and dried to give the chloride salt (52 mg). This solid was dissolved in a minimum of methanol and aqueous $[NBu^n{}_4]I$ was added. Diethyl ether was then added and the purple precipitate was filtered off, washed with diethyl ether and dried. Yield: 52 mg (72%). δ_H (CD_3OD) 9.89 (d, 4H, J = 7.3 Hz, C_5H_4N), 9.11 (d, 4H, J = 4.8 Hz, $C_4N_2H_3$), 8.35–8.26 (8H, CH, C_5H_4N and $C_{10}H_5$), 8.06 (d, 2H, J = 9.8 Hz, $C_{10}H_5$), 7.81 (t, 2H, J = 4.8 Hz, $C_4N_2H_3$), 7.73 (d, 2H, J = 10.8 Hz, $C_{10}H_5$), 7.60–7.56 (4H, CH and $C_{10}H_5$), 7.21 (d, 2H, J = 8.8 Hz, $C_{10}H_5$), 2.61 (s, 12H, Me). m/z = 353 ($[M - 2I]^{2+}$). Anal. Calcd (%) for $C_{46}H_{40}I_2N_8{\bullet}3H_2O$: C, 54.56; H, 4.58; N, 11.06. Found; C, 54.83; H, 4.49; N, 10.57.

2.4. *X-ray crystallographic studies*

The data were collected by using a Bruker APEX CCD X-ray diffractometer using graphite-monochromated, MoKα radiation (wavelength = 0.71073 Å). Data processing was carried out by using the Bruker SAINT [12] software package and a semi-empirical absorption correction was applied by using SADABS [12]. The structures were solved by direct methods and refined by full-matrix least-squares on all F_0^2 data using SHELXS 97 [13] and SHELXL 97 [14]. All non-hydrogen atoms were refined anisotropically, with hydrogen atoms bonded to carbon or nitrogen included in calculated positions using the riding method. All other calculations were carried out by using the SHELXTL package [15]. Crystallographic data and refinement details are presented in Table 1. The CCDC depositions 761 448 and 761 449 contain the supplementary crystallographic data for this paper. These data can be obtained free of charge via www.ccdc.cam.ac.uk/data_request/cif, data_request@ccdc.cam.ac.uk, or by contacting The Cambridge Crystallographic Data Centre, 12, Union Road, Cambridge CB2 1EZ, UK; fax: +44 1223 336033.

Table 1
Crystallographic data and refinement details for compounds **2** and **3**.

	2	**3**
Empirical formula	$C_{24}H_{22}Br_2N_2$	$C_{26}H_{24}N_2O_2$
fw	498.26	396.47
Appearance	white plate	yellow needle
Cryst size/mm	0.20 × 0.15 × 0.10	0.50 × 0.15 × 0.15
Cryst syst	orthorhombic	orthorhombic
Space group	$P2_12_12_1$	$P2_12_12_1$
a/Å	7.2839(9)	8.7933(7)
b/Å	8.7125(10)	14.9796(12)
c/Å	32.703(4)	15.7605(13)
U/Å^3	2075.4(4)	2076.0(3)
Z	4	4
T/K	100(2)	100(2)
μ/mm^{-1}	3.918	0.081
Reflns collected	16675	16657
Independent reflns (R_{int})	4262(0.0515)	2420(0.0690)
GOF on F^2	1.118	1.004
Final R1, wR2 [$I > 2\sigma(I)$][a]	0.0437, 0.0773	0.0384, 0.0762
Final R1, wR2 (all data)	0.0516, 0.0813	0.0495, 0.0792

[a] The structures were refined on F_o^2 using all data; the value of $R1$ is given for comparison with older refinements based on F_o with a typical threshold of $F_o > 4\sigma(F_o)$.

2.5. *Hyper-Rayleigh scattering*

The apparatus and experimental procedures used for the fs HRS studies were exactly as described previously [16]. All measurements were carried out in acetonitrile and the reference compounds were Disperse Red 1 ($\beta_{1300} = 86 \times 10^{-30}$ esu in acetonitrile; from the value of 54×10^{-30} esu in chloroform, corrected for local field factors at optical frequencies) or crystal violet ($\beta_{800} = 327 \times 10^{-30}$ esu in acetonitrile; from the value of 338×10^{-30} esu in methanol, corrected for local field factors at optical frequencies). Dilute solutions (10^{-5} to 10^{-6} M) were used to ensure a linear dependence of $I_{2\omega}/I_{\omega}^2$ on concentration, precluding the need for Lambert–Beer correction factors. The absence of demodulation at both 800 and 1300 nm, i.e. constant values of β versus amplitude modulation frequency, showed that no fluorescence contributions to the HRS signals were present at these measurement wavelengths. This situation may indicate: *(i)* a lack of fluorescence, *(ii)* spectral filtering out of fluorescence, or *(iii)* the fluorescence lifetime is too short for its demodulation to be observed within the bandwidth of the instrument. The reported β values are the averages taken from measurements at different amplitude modulation frequencies.

3. Results and discussion

3.1. *Synthesis and characterisation*

The reaction chemistry used to prepare the new compounds is depicted in Scheme 1. The known compound **1**, derived from bromination of commercial (*R*)-1,1′-binaphthalenyl-2,2′-diamine [8], is methylated using slight modification of a published procedure [17] to give **2**. The isolated yield of 51% is similar to that reported for a related preparation of the corresponding tetra(*n*-butyl) compound [8], although literature reports of similar reactions with (*R*)-1,1′-binaphthalenyl-2,2′-diamine document yields of *ca*. 85–88% [17c,d,18]. The bromine atoms in **2** are replaced with aldehyde groups by using lithiation followed by a DMF quench to give **3** in 55% isolated yield after column chromatography on silica gel. The same approach was used previously by Koeckelberghs et al. to prepare the 2,2′-di(*n*-hexyloxy) analogue of **3** in a slightly higher yield [6k], although the latter was isolated as an oil while **3** is a yellow crystalline solid.

Our original intention was to use **3** to synthesise cations **5**–**7** via Knoevenagel-type condensation reactions, as used previously to prepare related pseudo-linear chromophores [9a,c]. A reaction was performed between **3** and *N*-methyl-4-picolinium iodide in methanol with piperidine as a base; heating under reflux for 4 h gave a diagnostic colour change from pale yellow to deep red. The crude iodide salt was obtained and metathesised to its

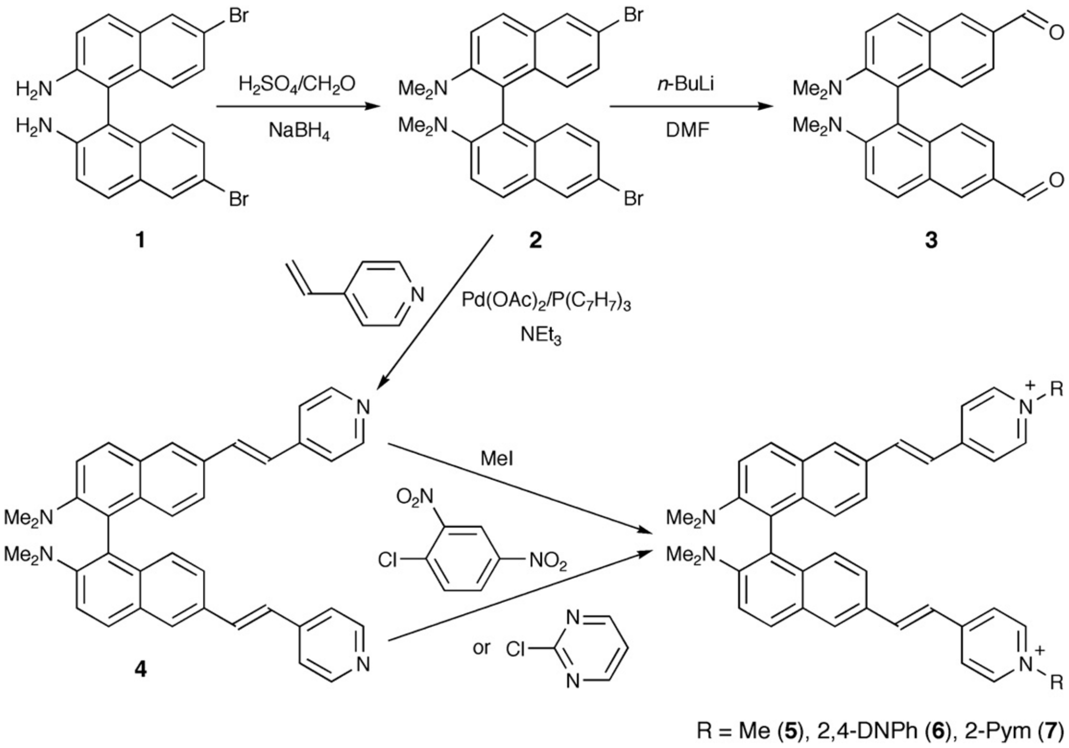

Scheme 1. Strategy for the syntheses of compounds **2**–**4** and cations **5**–**7**.

hexafluorophosphate counterpart, [**5**]PF_6. However, the ^1H NMR spectrum recorded in CD_3COCD_3 showed the presence of the desired chromophore, but with several impurity peaks at a *ca.* 20% level. These unwanted signals are similar to those of the product, but shifted upfield. The presence of a doublet at 6.90 ppm with a *J* value of 8.9 Hz is indicative of the formation of (*Z*)-isomer(s) as well as the desired (*E*,*E*)-product. It is noteworthy that the spectrum that Yan et al. obtained for the related cation **8** (Fig. 1) also shows minor signals that are attributable to the (*Z*)-isomer(s) [8].

Since we were unable to separate the isomers of **5** via recrystallisation or chromatography, an alternative synthetic route was adopted using a Heck cross-coupling reaction, as used by Yan et al. to produce the tetra(*n*-butyl) analogue of **4** [8]. **4** was thus isolated in 50% yield after column chromatography on silica gel as only its (*E*,*E*)-isomer. Treatment of **4** with methyl iodide then afforded [**5**]I_2 in 79% yield, with the ^1H NMR spectrum (Fig. 2) showing no trace of the (*Z*)-isomer(s).

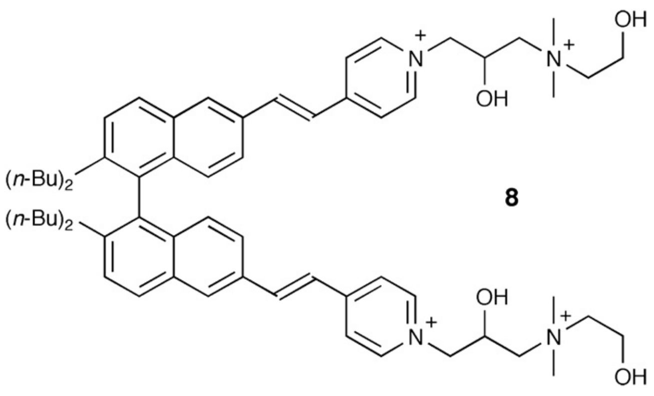

Fig. 1. Structure of a dicationic 1,1′-binaphthalenyl chromophore reported by Yan et al. previously [8].

[**5**]I_2 was dissolved in methanol and metathesised to its hexafluorophosphate salt, as solubility in acetone or acetonitrile is generally desirable for NLO measurements. The ^1H NMR spectrum of [**5**]$[PF_6]_2$ recorded in CD_3COCD_3 again showed the presence of the (*Z*)-isomer(s). Although facile photo-isomerisation of related compounds is well precedented [19], NMR samples of [**5**]I_2 in CD_3OD show no evidence for isomerisation after exposure to room lighting for periods of up to 72 h. In addition, metathesis to [**5**]$[PF_6]_2$ leads to isomerisation even when the sample is kept in the dark, but the minor signals do not gain in intensity following exposure to light in CD_3COCD_3. These observations indicate that the isomerisation of **5** is not photo-activated, but occurs thermally and is strongly influenced by changes in the solvent medium.

The 2,4-dinitrophenyl (2,4-DNPh) and 2-pyrimidyl (2-Pym)-functionalised cations **6** and **7** were also synthesised from **4** via straightforward S_NAr reactions, giving 72% isolated yields of the salts [**6**]Cl_2 and [**7**]I_2. The ^1H NMR spectra of the products in CD_3OD display dominant signals for the desired chromophores, but small peaks reveal the presence of the (*Z*)-isomers at levels of *ca.* 5–10%, especially doublets at 6.93 ppm ($J = 9.1$ Hz) for [**6**]Cl_2 and 7.07 ppm ($J = 9.6$ Hz) for [**7**]I_2. These spectra remained unchanged after exposure to room lighting for up to 72 h. The CHN elemental analyses for these samples fit satisfactorily, consistent with the likelihood that

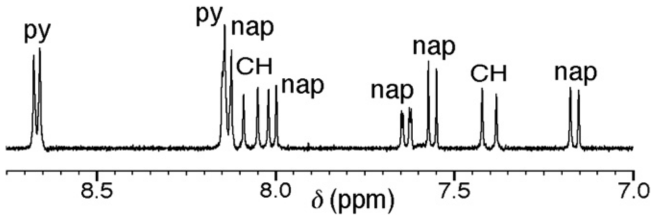

Fig. 2. Aromatic region of the ^1H NMR spectrum of [**5**]I recorded in CD_3OD at 400 MHz (py = pyridyl; nap = naphthalenyl).

the impurities are isomers. It is probable that the synthetic approaches used give rise to greater degrees of isomerisation for **6** and **7** when compared with **5** because the former are prepared under more forcing conditions (reflux at 80 °C in 2-butanone for 24 or 17 h, as opposed to reflux at 56 °C in acetone for 4 h). Attempts to prepare **6** and **7** in acetone were unsuccessful and it thus appears that some degree of (*E*) → (*Z*) isomerism is unavoidable for these chromophores. However, because the (*Z*)-isomers are present in only small proportions, the optical measurements were nevertheless performed on these samples (see below), on the assumption that the low levels of (*Z*)-isomers present will not affect the results appreciably.

3.2. Electronic absorption spectroscopy

The UV–vis absorption spectra of salts [**5**]I_2, [**6**]Cl_2 and [**7**]I_2 have been measured in methanol and the results are presented in Table 2. These spectra are dominated by intense $\pi \rightarrow \pi^*$ intramolecular charge-transfer (ICT) bands in the visible region and also one or more intense bands due to $\pi \rightarrow \pi^*$ transitions having less directionality at higher energies. Representative spectra are shown in Fig. 3.

Moving along the series **5**–**7**, the energy of the ICT band decreases steadily in the order R = Me > 2,4-DNPh > 2-Pym, with a total red-shift of 0.38 eV between the extremes. This pattern is attributable to the increasing electron-withdrawing strength of the pyridinium group, as observed previously with related 1D dipolar chromophores [9]. The lowest energy UV band shows the same red-shifting trend, although the total decrease in E_{max} (0.28 eV) is smaller than that observed for the ICT absorptions. While the intensity of the ICT band is essentially independent of R, that of the first UV absorption increases substantially in the order R = Me < 2-Pym < 2,4-DNPh, with a *ca.* 50% increase in molar extinction coefficient on moving from [**5**]I_2 to [**6**]Cl_2.

3.3. X-ray crystallography

Single crystal X-ray structures of the compounds **2** and **3** have been obtained and representations of their molecular structures can be seen in Figs. 4 and 5. Selected crystallographic and refinement details are shown in Table 1 and selected bond lengths in Table 3. Both compounds adopt the noncentrosymmetric space group $P2_12_12_1$, a logical consequence of their resolved chiral nature. The respective dihedral angles between the two naphthalenyl rings in **2** and **3** are 75.03° and 70.67°, as expected due to pronounced steric interactions, especially between the $-NMe_2$ substituents. The bond lengths within the naphthalenyl rings show the expected variations based upon the contributions of three resonance forms making distances 2, 6, 8 and 10 shorter than the other six C–C distances by as much as *ca.* 0.08 Å. Similar effects are also observed in the known compounds (*R*)-2,2′-diamino-1,1′-binaphthalenyl [20] and (*R*)-2,2′-bis(dimethylamino)-1,1′-binaphthalenyl [21]. All of these bond lengths are invariant between **2** and **3**, showing that the electronic effects of the bromo and formyl substituents are indistinguishable. The N–Me distances also show some small but significant variations, being on average shorter in **2** when compared with **3** (1.422 vs. 1.448 Å).

Table 2
UV–vis absorption data for [**5**]I_2, [**6**]Cl_2 and [**7**]I_2 in methanol at 293 K.

Salt	λ_{max}, nm (ε, 10^3 M^{-1} cm^{-1})[a]	E_{max}, eV	Assignment
[**5**]I_2	460 (41.8)	2.70	ICT
	331 (29.6)	3.75	$\pi \rightarrow \pi^*$
	257 (34.1)	4.82	$\pi \rightarrow \pi^*$
[**6**]Cl_2	519 (41.7)	2.39	ICT
	352 (44.8)	3.52	$\pi \rightarrow \pi^*$
[**7**]I_2	534 (42.6)	2.32	ICT
	357 (39.7)	3.47	$\pi \rightarrow \pi^*$
	261 (57.0)	4.75	$\pi \rightarrow \pi^*$

[a] Solutions *ca.* 10^{-5} M.

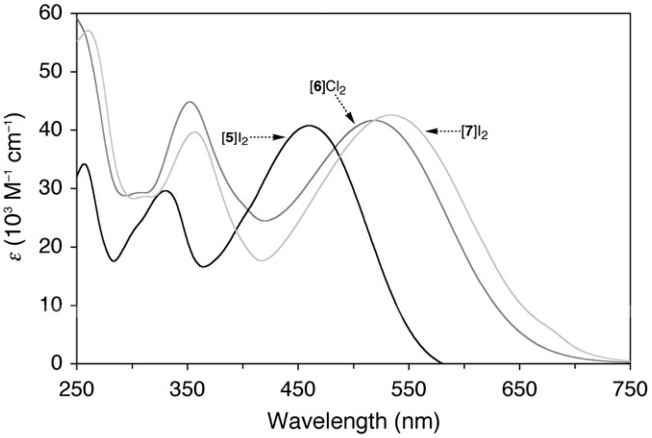

Fig. 3. UV–vis absorption spectra of [**5**]I_2 (black), [**6**]Cl_2 (grey) and [**7**]I_2 (light grey) at 293 K in acetonitrile.

3.4. Hyper-Rayleigh scattering

The HRS technique has been used to determine β values for the new chromophores **5**–**7** using both 800 and 1300 nm laser fundamentals and the results of these measurements are presented in Table 4. Because these compounds absorb much more strongly at the second harmonic wavelength 400 when compared with 650 nm, the β_{HRS} values measured using the 800 nm laser are enhanced by resonance to a greater extent.

For 1D dipolar molecules, the hyperpolarizability has a single dominant tensor component along the charge-transfer (z) axis, β_{zzz}. For a 2D dipolar molecule with two planar subunits, z corresponds with the two-fold axis and there are two independent tensor components, β_{zzz} and β_{zxx}, which can be expressed as a function of

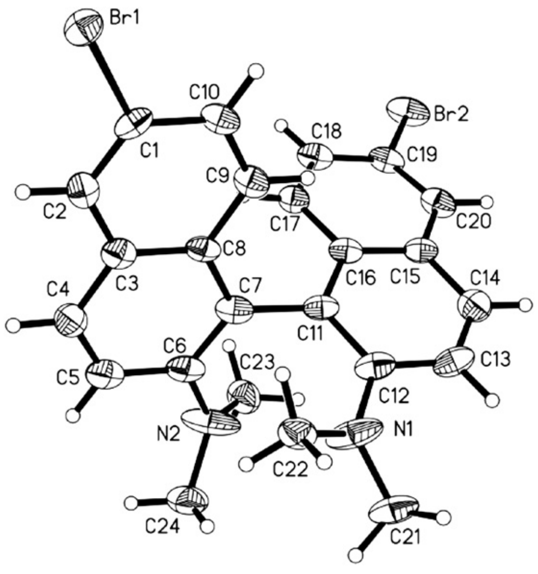

Fig. 4. Representation of the molecular structure of **2** (50% probability ellipsoids).

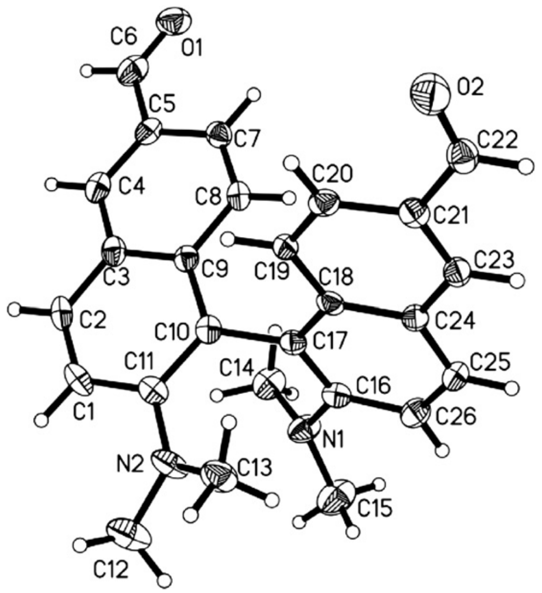

Fig. 5. Representation of the molecular structure of **3** (50% probability ellipsoids).

the dihedral angle θ between the subunits, according to equations (1) and (2). We have thus derived values of β_{zzz} and β_{zxx} for **5**–**7**, using a rounded average of the dihedral angles observed crystallographically for **2** and **3** (see above), assuming that the dihedral angles for **5**–**7** in solution will be similar. The results are also shown in Table 4. Previous studies have shown that 2D dipolar chromophores are of special interest for potential NLO applications because they can avoid reabsorption of second harmonic light and also achieve phase-matching of second harmonic generation due to polarization effects [22].

Table 3
Selected interatomic distances (Å) for compounds **2** and **3.**

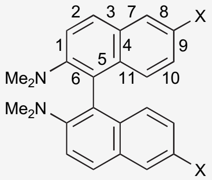	2		3	
N–C(Me)	1.422(6)	1.439(6)	1.449(3)	1.446(3)
N–C(Me)	1.398(6)	1.429(6)	1.456(3)	1.440(3)
N–C(nap)	1.402(6)	1.402(6)	1.386(3)	1.385(3)
C–C(1)	1.422(7)	1.415(7)	1.419(3)	1.430(3)
C–C(2)	1.354(7)	1.358(7)	1.358(3)	1.354(3)
C–C(3)	1.421(7)	1.423(7)	1.424(3)	1.420(3)
C–C(4)	1.424(6)	1.406(6)	1.425(3)	1.425(3)
C–C(5)	1.430(6)	1.435(6)	1.421(3)	1.420(3)
C–C(6)	1.383(7)	1.400(6)	1.405(3)	1.402(3)
C–C(7)	1.405(6)	1.415(6)	1.406(3)	1.401(3)
C–C(8)	1.361(6)	1.354(7)	1.372(3)	1.372(3)
C–C(9)	1.401(6)	1.397(6)	1.414(3)	1.414(3)
C–C(10)	1.363(6)	1.372(6)	1.362(3)	1.361(3)
C–C(11)	1.421(6)	1.419(6)	1.428(3)	1.432(3)
C–X(X=Br/CHO)	1.909(4)	1.902(4)	1.462(3)	1.464(3)
C–O	–	–	1.212(3)	1.214(3)

Table 4
HRS data for [**5**]I_2, [**6**]Cl_2 and [**7**]I_2 in methanol at 293 K.

Salt	800 nm (10^{-30} esu)			1300 nm (10^{-30} esu)		
	β_{HRS}[a]	β_{zzz}[b]	β_{zxx}[c]	β_{HRS}[d]	β_{zzz}[e]	β_{zxx}[f]
[**5**]I_2	117 ± 7	194	106	34 ± 3	56	31
[**6**]Cl_2	126 ± 5	209	114	83 ± 10	138	76
[**7**]I_2	155 ± 9	257	141	91 ± 12	151	83

[a] Dynamic first hyperpolarizability measured using a 800 nm laser.
[b] Derived from 800 nm β_{HRS} value by using equation (1).
[c] Derived from 800 nm β_{zzz} value by using equation (2) with $\theta = 73°$.
[d] Dynamic first hyperpolarizability measured using a 1300 nm laser.
[e] Derived from 1300 nm β_{HRS} value by using equation (1).
[f] Derived from 1300 nm β_{zzz} value by using equation (2) with $\theta = 73°$. The esu units can be converted to SI units ($C^3\,m^3\,J^{-2}$) by dividing by a factor of 2.693×10^{-20}.

Moving along the series **5**–**7**, the β_{HRS} values measured at 800 and 1300 nm increase steadily as the electron acceptor strength increases, and the same is true of the tensor components β_{zzz} and β_{zxx}. This trend is consistent with the visible spectroscopic data (see above) in the context of the standard two-state model which states that the β response generally increases as the associated ICT energy decreases [23]. As defined by equation (2), for all of the measurements, the β_{zxx} values are *ca.* 0.55 times the β_{zzz} components. Hence for these molecules the largest proportion of the total hyperpolarizability lies along the charge-transfer axis, but the "off-diagonal" β_{zxx} tensor components are still substantial and larger when compared to those determined by HRS for other 2D dipoles in the literature. A series of ruthenium(II) tetraammine complexes with pyridinium electron acceptor groups shows β_{zyy} values in the range 50–60 × 10^{-30} esu, measured using a 800 nm laser [24]. Related 1,1′-binaphthalenyl chromophores show β_{zxx} values in the range 3–10 × 10^{-30} esu [6c], and the 2D 3,6-dinitro-9-ethylcarbazole [25] has $\beta_{zxx} \approx 19 \times 10^{-30}$ esu, all measured using a 1064 nm laser. Given the relative magnitudes and significant 2D nature of their β responses, **5**–**7** are promising candidates for bulk NLO studies if they can be incorporated into suitable polar structures.

$$\left\langle \beta_{HRS}^2 \right\rangle = \left(\frac{6}{35}+\frac{16}{105}\left(\tan\frac{\theta}{2}\right)^2+\frac{38}{105}\left(\tan\frac{\theta}{2}\right)^4\right)\beta_{zzz}^2 \tag{1}$$

$$\beta_{zxx} = \left(\tan\frac{\theta}{2}\right)^2\beta_{zzz} \tag{2}$$

4. Conclusions

We have synthesised and characterised three new 2D dipolar cations as their resolved *R* enantiomers. The intense, visible ICT bands of these chromophores red-shift as the electron acceptor strength increases, as observed previously with related 1D species. Femtosecond HRS measurements with 1300 and 800 nm lasers afford β values in the range 34–155 × 10^{-30} esu that show the expected inverse relationship with respect to the ICT energies. Single crystal X-ray structures for the precursor compounds **2** and **3** show an average dihedral angle θ between the naphthalenyl units of 73°. Assuming a similar θ value for the chromophores **5**–**7** in solution allows the determination of two independent tensor components, β_{zzz} and β_{zxx}. In all cases, β_{zzz} is dominant, but the "off-diagonal" β_{zxx} values are nevertheless substantial (31–141 × 10^{-30} esu) and larger than those determined by HRS for other 2D dipoles previously. Crystallisation of cations **5**–**7** with appropriate anions will afford noncentrosymmetric structures that may show large bulk NLO effects if the dipoles align favourably.

Acknowledgment

We thank the EPSRC for support in the form of a PhD studentship (ECH), and also the Fund for Scientific Research-Flanders (FWO-V, G.0312.08) and the University of Leuven (GOA/2006/3).

We are also grateful to Dr Madeleine Helliwell (University of Manchester) for assistance with the X-ray crystallography and to Dr Inge Asselberghs (University of Leuven) for advice concerning the HRS measurements.

References

[1] (a) Chemla DS, Zyss J, editors. Nonlinear optical properties of organic molecules and crystals, vols. 1 and 2. Orlando, FL: Academic Press; 1987;
(b) Zyss J. Molecular nonlinear optics: materials, physics and devices. Boston: Academic Press; 1994;
(c) Bosshard Ch, Sutter K, Prêtre Ph, Hulliger J, Flörsheimer M, Kaatz P, et al. Organic nonlinear optical materials. In: Advances in nonlinear optics, vol. 1. Amsterdam, The Netherlands: Gordon & Breach; 1995;
(d) Nalwa HS, Miyata S, editors. Nonlinear optics of organic molecules and polymers. Boca Raton, FL: CRC Press; 1997;
(e) Papadopoulos MG, Leszczynski J, Sadlej AJ, editors. Nonlinear optical properties of matter: from molecules to condensed phases. Dordrecht: Springer; 2006.

[2] (a) Marder SR, Perry JW, Schaefer WP. Synthesis of organic salts with large second-order optical nonlinearities. Science 1989;245:626–8;
(b) Marder SR, Perry JW, Schaefer WP. 4-N-methylstilbazolium toluene-p-sulfonate salts with large second-order optical non-linearities. J Mater Chem 1992;2:985–6;
(c) Marder SR, Perry JW, Yakymyshyn CP. Organic salts with large second-order optical nonlinearities. Chem Mater 1994;6:1137–47;
(d) Lee O-K, Kim K-S. NLO materials based on stilbazolium salt chromophores. Photonics Sci News 1999;4:9–20;
(e) Sohma S, Takahashi H, Taniuchi T, Ito H. Organic nonlinear optical crystal DAST growth and its device applications. Chem Phys 1999;245:359–64;
(f) Kaino T, Cai B, Takayama K. Fabrication of DAST channel optical waveguides. Adv Funct Mater 2002;12:599–603;
(g) Mohan Kumar R, Rajan Babu D, Ravi G, Jayavel R. Growth and characterization of 4-dimethylamino-N-methyl-4-stilbazolium tosylate (DAST) single crystals. J Cryst Growth 2003;250:113–7;
(h) Geis W, Sinta R, Mowers W, Deneault SJ, Marchant MF, Krohn KE, et al. Fabrication of crystalline organic waveguides with an exceptionally large electro-optic coefficient. Appl Phys Lett 2004;84:3729–31.

[3] (a) Yitzchaik S, Marks TJ. Chromophoric self-assembled superlattices. Acc Chem Res 1996;29:197–202;
(b) Alain V, Blanchard-Desce M, Ledoux-Rak I, Zyss J. Amphiphilic polyenic push–pull chromophores for nonlinear optical applications. Chem Commun; 2000:353–4;
(c) Cariati E, Ugo R, Cariati F, Roberto D, Masciocchi N, Galli S, et al. J-aggregates granting giant second-order NLO responses in self-assembled hybrid inorganic-organic materials. Adv Mater 2001;13:1665–8;
(d) Abbotto A, Beverina L, Bradamante S, Facchetti A, Klein C, Pagani GA, et al. A distinctive example of the cooperative interplay of structure and environment in tuning of intramolecular charge transfer in second-order nonlinear optical chromophores. Chem–Eur J 2003;9:1991–2007;
(e) Kim HS, Lee SM, Ha K, Jung C, Lee Y-J, Chun YS, et al. Aligned inclusion of hemicyanine dyes into silica zeolite films for second harmonic generation. J Am Chem Soc 2004;126:673–82;
(f) Yang Z, Aravazhi S, Schneider A, Seiler P, Jazbinšek M, Günter P. Synthesis and crystal growth of stilbazolium derivatives for second-order nonlinear optics. Adv Funct Mater 2005;15:1072–6;
(g) Ruiz B, Yang Z, Gramlich V, Jazbinšek M, Günter P. Synthesis and crystal structure of a new stilbazolium salt with large second-order optical nonlinearity. J Mater Chem 2006;16:2839–42;
(h) Kim HS, Sohn KW, Jeon Y, Min H, Kim D, Yoon KB. Aligned inclusion of *n*-propionic acid tethering hemicyanine into silica zeolite film for second harmonic generation. Adv Mater 2007;19:260–3;
(i) Yang Z, Jazbinšek M, Ruiz B, Aravazhi S, Gramlich V, Günter P. Molecular engineering of stilbazolium derivatives for second-order nonlinear optics. Chem Mater 2007;19:3512–8.

[4] (a) Kawase K, Mizuno M, Sohma S, Takahashi H, Taniuchi T, Urata Y, et al. Difference-frequency terahertz-wave generation from 4-dimethylamino-N-methyl-4-stilbazolium-tosylate by use of an electronically tuned Ti:sapphire laser. Opt Lett 1999;24:1065–7;
(b) Kawase K, Hatanaka T, Takahashi H, Nakamura K, Taniuchi T, Ito H. Tunable terahertz-wave generation from DAST crystal by dual signal-wave parametric oscillation of periodically poled lithium niobate. Opt Lett 2000;25:1714–6;
(c) Taniuchi T, Okada S, Nakanishi H. Widely tunable terahertz-wave generation in an organic crystal and its spectroscopic application. Appl Phys Lett 2004;95:5984–8;
(d) Taniuchi T, Ikeda S, Okada S, Nakanishi H. Tunable sub-terahertz wave generation from an organic DAST crystal. Jpn J Appl Phys 2005;44:L652–4;
(e) Schneider A, Neis M, Stillhart M, Ruiz B, Khan RUA, Günter P. Generation of terahertz pulses through optical rectification in organic DAST crystals: theory and experiment. J Opt Soc Am B 2006;23:1822–35;
(f) Schneider A, Stillhart M, Günter P. High efficiency generation and detection of terahertz pulses using laser pulses at telecommunication wavelengths. Opt Express 2006;14:5376–84;
(g) Yang Z, Mutter L, Stillhart M, Ruiz B, Aravazhi S, Jazbinšek M, et al. Large-size bulk and thin-film stilbazolium-salt single crystals for nonlinear optics and THz generation. Adv Funct Mater 2007;17:2018–23.

[5] Andreu R, Malfant I, Lacroix PG, Gornitzka H, Nakatani K. Chiral stilbazolium chromophores: an approach toward multiproperty materials combining conductivity and second-order optical nonlinearities. Chem Mater 1999;11:840–8.

[6] (a) Wong MS, Nicoud J-F. Synthesis of novel non-centrosymmetric crystalline materials for quadratic non-linear optics. J Chem Soc, Chem Commun; 1994:249–50;
(b) Deussen H-J, Hendrickx C, Boutton C, Krog D, Clays K, Bechgaard K, et al. Novel chiral bis-dipolar 6,6′-disubstituted binaphthol derivatives for second-order nonlinear optics: synthesis and linear and nonlinear optical properties. J Am Chem Soc 1996;118:6841–52;
(c) Hendrickx E, Boutton C, Clays K, Persoons A, van Es S, Biemans T, et al. Quadratic nonlinear optical properties of correlated chromophores: cyclic 6,6′-dinitro-1,1′-binaphthyl-2,2′-ethers. Chem Phys Lett 1997;270:241–4;
(d) Deussen H-J, Boutton C, Thorup N, Geisler T, Hendrickx E, Bechgaard K, et al. New chiral bis(dipolar) 6,6′-disubstituted binaphthol derivatives for second-order nonlinear optics. Chem–Eur J 1998;4:240–50;
(e) Zrig S, Koeckelberghs G, Verbiest T, Andrioletti B, Rose E, Persoons A, et al. Λ-Type regioregular oligothiophenes: synthesis and second-order NLO properties. J Org Chem 2007;72:5855–8;
(f) Van Elshocht S, Verbiest T, Kauranen M, Ma L, Cheng H, Musick KY, et al. Chiral 1,1′-binaphthyl-based helical polymers as nonlinear optical materials. Chem Phys Lett 1999;309:315–20;
(g) Koeckelberghs G, Sioncke S, Verbiest T, Persoons A, Samyn C. Synthesis and properties of chiral helical chromophore-functionalised polybinaphthalenes for second-order nonlinear optical applications. Polymer 2003;44:3785–94;
(h) Koeckelberghs G, Sioncke S, Verbiest T, Persoons A, Samyn C. Synthesis and properties of chiral donor-embedded polybinaphthalenes for nonlinear optical applications. Chem Mater 2003;15:2870–2;
(i) Koeckelberghs G, Vangheluwe M, Picard I, De Groof L, Verbiest T, Persoons A, et al. Synthesis and properties of new chiral donor-embedded polybinaphthalenes for nonlinear optical applications. Macromolecules 2004;37:8530–7;
(j) Koeckelberghs G, Verbiest T, Vangheluwe M, De Groof L, Asselberghs I, Picard I, et al. Influence of monomer optical purity on the conformation and properties of chiral, donor-embedded polybinaphthalenes for nonlinear optical purposes. Chem Mater 2005;17:118–21;
(k) Koeckelberghs G, De Groof L, Picard I, Verbiest T, Persoons A, Samyn C. Donor-embedded polybinaphthalenes for nonlinear optical applications: influence of the incorporation of a double bond. Macromol Rapid Commun 2005;26:905–10.

[7] Hudson RDA, Manning AR, Gallagher JF, Garcia MH, Lopes N, Asselberghs I, et al. Chiral organometallic chromophores for nonlinear optics derived from $[Fe_2(\eta^5\text{-}C_5H_5)_2(CO)_2(\mu\text{-}CO)(\mu\text{-}C\text{–}CH_3)]^+$ $[BF4]^-$. J Organomet Chem 2002;655:70–88.

[8] Yan P, Millard AC, Wei M, Loew LM. Unique contrast patterns from resonance-enhanced chiral SHG of cell membranes. J Am Chem Soc 2006;128:11030–1.

[9] (a) Coe BJ, Harris JA, Asselberghs I, Clays K, Olbrechts G, Persoons A, et al. Quadratic nonlinear optical properties of N-aryl stilbazolium dyes. Adv Funct Mater 2002;12:110–6;
(b) Clays K, Coe BJ. Design strategies versus limiting theory for engineering large second-order nonlinear optical polarizabilities in charged organic molecules. Chem Mater 2003;15:642–8;
(c) Coe BJ, Harris JA, Asselberghs I, Wostyn K, Clays K, Persoons A, et al. Quadratic optical nonlinearities of *N*-methyl and *N*-aryl pyridinium salts. Adv Funct Mater 2003;13:347–57;
(d) Coe BJ, Beljonne D, Vogel H, Garín J, Orduna J. Theoretical analyses of the effects on the linear and quadratic nonlinear optical properties of *N*-arylation of pyridinium groups in stilbazolium dyes. J Phys Chem A 2005;109:10052–7.

[10] Figi H, Mutter L, Hunziker C, Jazbinšek M, Günter P, Coe BJ. Extremely large nonresonant second-order nonlinear optical response in crystals of the stilbazolium salt DAPSH. J Opt Soc Am B 2008;25:1786–93.

[11] (a) Clays K, Persoons A. Hyper-Rayleigh scattering in solution. Phys Rev Lett 1991;66:2980–3;
(b) Hendrickx E, Clays K, Persoons A. Hyper-Rayleigh scattering in isotropic solution. Acc Chem Res 1998;31:675–83.

[12] SAINT (version 6.45) and SADABS (version 2.10). Madison: Wisconsin, USA: Bruker AXS Inc; 2003.

[13] Sheldrick GM. Phase annealing in *SHELX*-90: direct methods for larger structures. Acta Crystallogr Sect A 1990;46:467–73.

[14] Sheldrick GM. SHELXL 97, program for crystal structure refinement. Göttingen, Germany: University of Göttingen; 1997.

[15] SHELXTL (version 6.10). Madison: Wisconsin, USA: Bruker AXS Inc; 2000.

[16] (a) Olbrechts G, Strobbe R, Clays K, Persoons A. High-frequency demodulation of multi-photon fluorescence in hyper-Rayleigh scattering. Rev Sci Instrum 1998;69:2233–41;
(b) Olbrechts G, Wostyn K, Clays K, Persoons A. High-frequency demodulation of multi-photon fluorescence in long-wavelength hyper-Rayleigh scattering. Opt Lett 1999;24:403–5;
(c) Clays K, Wostyn K, Olbrechts G, Persoons A, Watanabe A, Nogi K, et al. Fourier analysis of the femtosecond hyper-Rayleigh scattering signal from ionic fluorescent hemicyanine dyes. J Opt Soc Am B 2000;17:256–65;

(d) Franz E, Harper EC, Coe BJ, Zahradnik P, Clays K, Asselberghs I. Benzathiazoliums and pyridiniums for second-order nonlinear optics. Proc SPIE–Int Soc Opt Eng 2008;6999. 699923–1–11.

[17] (a) Guimanini AG, Chiavari G, Musiani MM, Rossi E. N-Permethylation of primary and secondary aromatic amines. Synthesis; 1980:743–6;
(b) Smrčina M, Vyskočil S, Polívková J, Poláková J, Sejbal J, Hanuš V, et al. Axially chiral 1,1′-binaphthyls with non-identical groups in 2,2′-positions. Synthesis of the enantiomerically pure 2-hydroxy-2′-thiol and substituted 2-amino-2′-thiols. Tetrahedron: Asymmetry 1997;8:537–46;
(c) Vyskočil S, Smrčina M, Kočovský P. A facile synthesis of the enantiopure, nitrogen-substituted 2,2′-diamino-1,1′-binaphthyls as potential ligands for catalytic asymmetric reactions. Collect Czech Chem Commun 1998;63:515–9;
(d) Vyskočil S, Jaracz S, Smrčina M, Štícha M, Hanuš V, Polášek M, et al. Synthesis of N-alkylated and N-arylated derivatives of 2-amino-2′-hydroxy-1,1′-binaphthyl (NOBIN) and 2,2′-diamino-1,1′-binaphthyl and their application in the enantioselective addition of diethylzinc to aromatic aldehydes. J Org Chem 1998;63:7727–37.

[18] (a) Benson SC, Cai P, Colon M, Haiza MA, Tokles M, Snyder JK. Use of carboxylic acids as chiral solvating agents for the determination of optical purity of chiral amines by NMR spectroscopy. J Org Chem 1988;53:5335–41;
(b) Müller P, Boléa C. Carbenoid pathways in copper-catalyzed intramolecular cyclopropanations of phenyliodonium ylides. Helv Chim Acta 2001;84:1093–111.

[19] (a) Gaines Jr GL. Photoisomerization of stilbazolium chromophores with potential nonlinear optical applications. Angew Chem Int Ed Engl 1987;99:341–2;
(b) Ebbesen TW, Tokumaru K, Sumitani M, Yoshihara K. Charge transfer and cis-trans photoisomerization. J Phys Chem 1989;93:5453–7;
(c) Busby M, Hartl F, Matousek P, Towrie M, Vlček Jr A. Ultrafast excited state dynamics controlling photochemical isomerization of *N*-methyl-4-[*trans*-2-(4-pyridyl)ethenyl]pyridinium coordinated to a $\{\mathrm{Re}^{\mathrm{I}}(\mathrm{CO})_3(2,2'\text{-bipyridine})\}$ chromophore. Chem–Eur J 2008;14:6912–23.

[20] Jones MD, Almeida Paz FA, Davies JE, Johnson BFG. (*R*)-(+)-2,2′-diamino-1,1′-binaphthyl. Acta Crystallogr Sect E 2003;59:o910–2.

[21] Franzini L, Rosini C, Pasero M. Structure of (*R*)-*N*,*N*,*N*′,*N*′-tetramethyl-[1, l′-binaphthalene]-2,2′-diamine. Acta Crystallogr Sect C 1991;47:1259–61.

[22] Wortmann R, Krämer P, Glania C, Lebus S, Detzer N. Deviations from Kleinman symmetry of the second-order polarizability tensor in molecules with low-lying perpendicular electronic bands. Chem Phys 1993;173:99–108.

[23] (a) Oudar JL, Chemla DS. Hyperpolarizabilities of the nitroanilines and their relations to the excited state dipole moment. J Chem Phys 1977;66:2664–8;
(b) Oudar JL. Optical nonlinearities of conjugated molecules. stilbene derivatives and highly polar aromatic compounds. J Chem Phys 1977;67:446–57.

[24] Coe BJ, Harris JA, Jones LA, Brunschwig BS, Song K, Clays K, et al. Syntheses and properties of two-dimensional charged nonlinear optical chromophores incorporating redox-switchable *cis*-tetraammineruthenium(II) centers. J Am Chem Soc 2005;127:4845–59.

[25] Boutton C, Clays K, Persoons A, Wada T, Sasabe H. Second-order off-diagonal hyperpolarizability tensor components of substituted carbazoles by hyper-Rayleigh scattering depolarization measurements. Chem Phys Lett 1998;286:101–6.